Resonant Surface Magnetic X-Ray Diffraction from Co₃Pt(111)

S. Ferrer, P. Fajardo, F. de Bergevin,* J. Alvarez, X. Torrelles, H. A. van der Vegt,† and V. H. Etgens‡

European Synchrotron Radiation Facility, BP 220, 38043 Grenoble Cedex, France
(Received 4 March 1996)

Surface magnetic x-ray diffraction experiments have been done on the (111) surface of the ferromagnetic alloy Co_3Pt. This has been achieved by tuning the photon energy to the L_{III} absorption edge of Pt in order to benefit from the increased magnetic cross section at resonance. Analysis of the data reveals that the magnetism of the Pt atoms on the first atomic layer is smaller by about a factor of 2 than that of the Pt atoms in the bulk, the reason probably being the reduced Co concentration at the surface. [S0031-9007(96)00680-1]

The demonstration almost 25 years ago [1] of the possibility of using x rays to study the magnetic properties of solids has resulted in a continuously increasing number of experiments in a large variety of magnetic systems. Most of them have used x-ray beams from synchrotron sources since the intensities of the magnetic signals are weak: typically 5 or 6 orders of magnitude smaller than the intensities from charge scattering.

X-ray scattering from surfaces is a well-established technique for structural studies [2] that in most cases also takes advantage of the intense synchrotron beams since the intensities from surface charge scattering are usually around 6 orders of magnitude weaker than those from the bulk of the material. The possibility of detecting magnetic scattering from surfaces presents the difficulty of measuring intensities around 11 or 12 orders of magnitude weaker than the normal bulk Bragg intensities. This is very demanding even for third generation synchrotron sources such as the ESRF. However, the discovery in 1988 [3] of the resonance exchange scattering which results in a large (2 orders of magnitude or more) increase of the magnetic signal when the photon energy is tuned to an absorption edge, makes the possibility of performing surface magnetic x-ray diffraction experiments realistic. This has been confirmed in previous experimental work [4,5] and it has also been discussed theoretically [6]. Very recently, Watson *et al.* [7] have also advanced in that direction of studying the magnetism of a surface region only a few nm thick. The present Letter represents a step forward since it provides direct evidence of the magnetism of the topmost atomic plane in a ferromagnetic surface.

A characteristic feature of surface x-ray scattering is that the diffracted intensities along straight lines in reciprocal space, normal to the surface of the crystal and passing through reciprocal lattice points where Bragg conditions are fulfilled, are not zero along the segments joining neighboring Bragg reflections. In these segments, the relatively weak intensities are sensitive to the structure of the surface. These "one-dimensional" distributions of intensity are designed as diffraction rods. We measured the diffracted intensities along several rods in order to determine the structure and stoichiometry of the surface of our alloy that was found to be Pt enriched. Next, we made similar measurements isolating the part of the diffracted intensity sensitive to the magnetization of the crystal. The structural results were used as input for the analysis of the magnetic measurements that revealed a depressed magnetic moment of the Pt atoms in the topmost atomic plane.

The experiments were performed on the surface diffraction beam line at ESRF that has been previously described in detail [8]. The Co_3Pt sample ($6 \times 10 \times 2$ mm³) was spark cut and polished to exhibit a (111) face (miscut ~0.1°). X-ray techniques were employed to verify the homogeneous composition and lattice parameter ($a_0 = 3.671$ Å). After insertion in the vacuum chamber, the surface was prepared with successive cycles of ion etching and annealing to 1200 K. The cleanliness of the surface was monitored with Auger electron spectroscopy. The crystal, which has the fcc structure, was not described with the standard cubic basis but instead with a hexagonal basis $\mathbf{a}_1, \mathbf{a}_2, \mathbf{a}_3$ with $\mathbf{a}_1$ and $\mathbf{a}_2$ in the surface plane ($a_1 = a_2 = a_0/\sqrt{2}$, nearest neighbor surface distance) and $\mathbf{a}_3$ perpendicular to the surface ($a_3 = \sqrt{3}\,a_0$). The corresponding reciprocal lattice vectors are directed along three axes H,K,L with H and K in the surface plane making an angle of 120° and L normal to the surface (see Ref. [9] for more details). The crystalline quality of the sample was examined by measuring the widths of bulk and surface reflections. Both bulk and surface mosaics had characteristics lengths of about 200 Å.

Crystallographic data were collected at an angle of incidence of twice the critical angle for total external reflection. After orienting the sample and detector to fulfill a (H,K,L) diffraction condition, the sample was rocked around its normal while measuring the scattered intensity. The intensity distributions were integrated and corrected by the appropriate geometrical factors (see Ref. [2]) to result in the magnitudes $|F_{HKL}|$ of the structure factors. Figure 1 shows the results for the rods $(1,0,L)$ and $(0,1,L)$ for $0.2 \leq L \leq 4$. The bulk Bragg peaks at $(1,0,1),(1,0,4)$, and $(0,1,2)$ appear as divergences in the figure. Two data sets crystallographically equivalent to the ones in the figure were measured in order to evaluate the error bars.
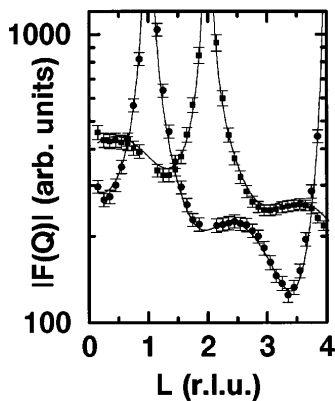
FIG. 1. The data points are the measured magnitudes of the structure factors of the rods $(1,0,L)$ (circles) and $(0,1,L)$ (squares) for different values of L. For clarity, the $(0,1,L)$ rod has been shifted upwards 100 units. The divergences at $L = 1, 2$, and 4 correspond to bulk Bragg reflections. The continuous curves are calculated with the structural model discussed in the text.

In a chemically ordered alloy, in addition to the so-called fundamental reflections arising from the translational symmetry of the crystal, there are the superstructure reflections which reflect the chemical ordering. The lack of measurable intensities in the superstructure reflections from our sample indicated the absence of long range chemical order. Thus the structure was modeled by assuming that the sample consisted in disordered bulk unit cells with the nominal stoichiometry and lattice parameter. The last three atomic planes parallel to the surface were allowed to differ from the bulk. They defined a disordered surface unit cell whose characteristic features were that the concentrations were allowed to be different in each layer and that the atomic coordinates of the atoms in the direction of the surface normal were allowed to relax. With all these compositional and structural hypotheses, a least squares fit was done to determine the structure. This results in Pt concentrations of the first three atomic planes (starting from the topmost one) equal to 0.60, 0.10, and 0.31, respectively. Also, it was found that the topmost layer is buckled since the Co atoms are displaced from their bulk position $(4.5 \pm 0.1)\%$ of a_3 outwards and the Pt atoms $(2 \pm 0.1)\%$ inwards. The second and third atomic layers exhibit relaxations smaller than 0.6%. The continuous curves in Fig. 2 are calculated with our structure model. As can be seen the agreement with the data is very good. To quantify it, the χ^2 parameter is commonly used [2]. Its value, 0.8 in our case, also indicates a good fit.

Our model agrees well with previously published [10] low-energy electron diffraction results in the same system which resulted in similar surface concentrations and relaxations.

Having determined the surface structural parameters, we concentrated in the magnetic measurements. The experiments were done by setting the photon energy at the L_{III} absorption edge of Pt (11.564 keV). Under these conditions, the scattering amplitude contains, in addition to the usual Thomson charge scattering f_0, significant contributions of the dispersive (f') and absorptive parts (f'') and a resonant magnetic term. Most of the experiments described below were done at grazing angles of incidence, typically at the critical angle $\alpha_c = 0.30°$. The direction of the scattered beam was defined with two angles as indicated in Fig. 2: the exit angle γ relative to the plane of the surface and the angle of in-plane scattering δ determined by the projection to the surface plane of the outgoing and incoming wave vectors. Under this geometry, if the sample is magnetized in the vertical direction and recalling that the incoming polarization is horizontal, one has for the scattering amplitude in units of r_0, the electron radius [11,12],

$$f = \cos\gamma(f_0 + f' - if'') + a_{\text{res}}, \quad (1)$$

$$a_{\text{res}} = \frac{i + x}{1 + x^2}(-n_p \cos\gamma - i\varepsilon n_m \sin\gamma \cos\delta). \quad (2)$$

n_p accounts for the white line at the absorption edge. Its numerical value is taken from Ref. [12] to be 4.3. ε may take the values 1 and -1 depending on the up or down orientation of the magnetization. x determines the relative energy deviation from resonance:

$$x = \frac{(E_f - E_i) - h\nu}{\Gamma/2}. \quad (3)$$

$E_f - E_i$ is the transition energy, $h\nu$ the energy of the photon, and Γ the width of the core level. The most important quantity is n_m, which is defined as the difference in the transition probabilities of dipolar transitions, from the core level to the Fermi energy, involving changes of angular momentum Δj_z of 1 and -1. A nonzero value of n_m in a magnetic atom arises from the spin splitting in the conduction band originated by the exchange interaction. In a somewhat loose sense, n_m may be visualized as being proportional to the magnetic moment of the resonant atom.

Expressions (1) and (2) are valid at zero incidence angles, which is a good approximation at the vicinities
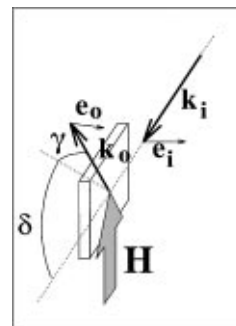

FIG. 2. Schematic layout of the geometry of the experiment. The sample surface lies in a vertical plane and is illuminated by the incoming wave vector $\mathbf{k}_i$ with polarization $\mathbf{e}_i$. The direction of the scattered wave vector $\mathbf{k}_0$ is determined by the angles γ and δ. $\mathbf{H}$ denotes the applied magnetic field that may be directed upwards or downwards.

of α_c. For arbitrary incidence angles the appropriate formulas [11,12] have to be used.

As may be seen from Eqs. (1) and (2), the diffracted intensity, which is proportional to $|f|^2$, will contain terms with odd parity in ε; therefore the asymmetry ratio

$$R = (I\uparrow - I\downarrow)/(I\uparrow + I\downarrow) \tag{4}$$

will be different from zero at the resonance energy ($x \approx 0$) where it exhibits a maximum. Away from resonance R decreases and the function $R(x)$ has a line shape that resembles a Lorentzian. Its detailed form has been discussed in Ref. [12] and will not be described here. In the previous paper by de Bergevin *et al.* [12], R was measured at resonance for different Bragg reflections in a CoPt ferromagnetic alloy. The measurements lead to $n_m = -0.8r_0$ for that sample.

Our experiments consisted of measuring R along diffraction rods. For this purpose a permanent NdFeB magnet was located inside the UHV chamber, at the vicinity of the surface of the Co_3Pt sample to create a magnetic field of 1.2 kG in the vertical direction as depicted in Fig. 2. The magnet could be rotated to invert the field direction and it could also be retrieved to allow surface preparation when needed.

Measuring the scattered intensity at the L_{III} resonance of Pt presents the difficulty that the signal at the detector contains, in addition to the elastically scattered photons, a fluorescent part arising from the core hole deexcitations with an energy only a few hundred eV lower. It constitutes a significant background that needs to be corrected from the data. To do so, two independent measurements were performed for determining the value of R at (H,K,L): one at the (H,K,L) position itself and another at a nearby position in reciprocal space. Usually the measurements were done by collecting first $I\uparrow$ and then $I\downarrow$ during the same time interval (1 min or less), then the same operation was repeated a number of times (from ~16 to ~64) to obtain a temporary averaged R value. Subsequently, the same routine of intensity collection was performed in the background often with the same duration in order to have reasonably low error bars in R.

Curve a in Fig. 3 shows the dependence of the asymmetry ratio with the photon energy in the proximity of the L_{III} absorption for the (006) reflection. It displays the expected resonant behavior. The energy width (FWHM) is of ~6 eV. By taking from Ref. [13] the value $\Gamma = 4$ eV as the energy width of the core hole, we deduce the energy distribution of our beam from the monochromator, which turns out to be described by a Gaussian energy distribution of standard deviation of 2 eV.

Before taking the measurements of R in the regions of the diffraction rods sensitive to the surface, we performed several measurements for different bulk Bragg reflections, namely, (104), (101), (-1,0,2), and (006). Their values of R at resonance ranged from $(2.7 \pm 0.6) \times 10^{-3}$ to $(30.5 \pm 0.4) \times 10^{-3}$.
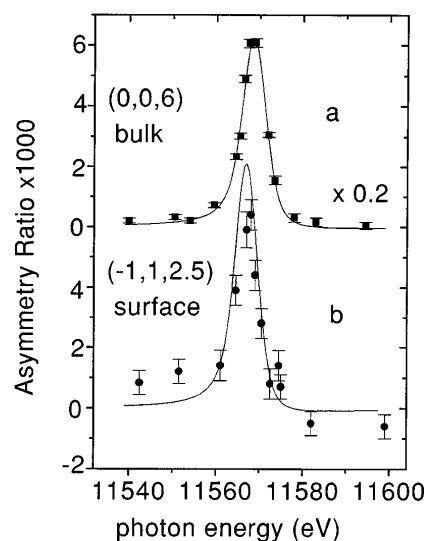

FIG. 3. Curve a: Asymmetry ratio vs photon energy at the vicinity of the Pt L_{III} absorption edge for the (006) bulk reflection. Curve b: The same for the $(-1,1,2.5)$ reflection, which has a very large surface sensitivity. The continuous curves are calculated as explained in the text.

With the help of the equations discussed above and taking as values of f' and f'' those of Ref. [12], one may evaluate n_m from the measurements of R made in the bulk Bragg peaks mentioned above. The result is $n_m = -0.9 \pm 0.1$ in very good agreement with the previously published value.

The data points of Fig. 3(b) are the measured values of R as a function of $h\nu$, at $(H,K,L) = (-1,1,2.5)$ which lies in between two neighboring bulk Bragg reflections $[(-1,1,1)$ and $(-1,1,4)]$ and the surface sensitivity is highest. The value at the maximum is $(6.4 \pm 0.5) \times 10^{-3}$. The continuous curve is a calculation with Eqs. (1) and (3) convoluted with the energy resolution. In the calculation, the atomic positions of the atoms in the topmost layer and the stoichiometry of the first three atomic planes have been taken from the structural model discussed above. The surface segregation of Pt is the main factor responsible for the small energy shift and for the increased asymmetric line shape of the surface resonance compared to the curve of the bulk. This arises from the structure factor expression rather than from a change in electronic structure at the surface. This will be discussed in more detail in a forthcoming publication.

In order to investigate the magnetic surface structure, measurements of R at resonance were performed for different values of L along a given diffraction rod. The data points in Fig. 4 are the results for the $(0,1,L)$ and $(1,0,L)$ rods. As can be seen, they have a rich structure consisting of several maxima and minima. The general trend of increase in R when L increases is due to the fact that at higher L values the exit angle γ is larger and the magnetic term in Eq. (3) becomes larger. The dashed vertical lines in the figure mark the positions of the bulk Bragg peaks.
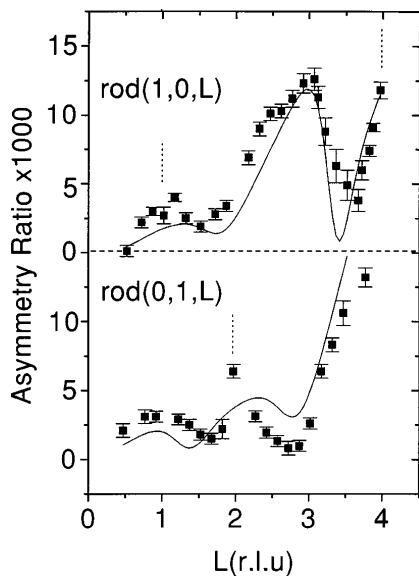
FIG. 4. Asymmetry ratio along the $(1,0,L)$ and $(0,1,L)$ diffraction rods for $0.5 \leq L \leq 4$. The dashed lines indicate the bulk reflections. The continuous curves are calculated by considering a reduced magnetic contribution of the topmost Pt atoms.

In order to find a model for the surface that fits the data, the crystallographic parameters of our structure model discussed above were taken as a fixed input and n_m was taken as the average value (-0.9) experimentally determined. We made the hypothesis that the Pt atoms of the topmost atomic layer could have a different value of n_m than the rest of the atoms. This ns_m was let as the only free parameter to fit the data in each of the rods of Fig. 4 and in the surface resonance curve of Fig. 3(b). The results of the calculations are displayed by the continuous curves. As may be seen, the quality of the fit to the data is good but not excellent. We suspect there are two main reasons for this. One is the simplicity of the model and the other is an experimental difficulty associated with the elongated shape of the crystal which causes an anisotropic surface demagnetizing field that might produce differences in the surface magnetization for different orientations of the surface.

The best fit value of ns_m is -0.43 ± 0.1 which is about a factor of 2 smaller than the bulk value. This indicates that the magnetic moment of the Pt atoms at the surface is reduced by the above factor compared to that of the bulk atoms. This is probably related to the fact that, due to the Pt surface segregation, the average number of Co nearest neighbors of a given Pt atom is a factor of 2 smaller for Pt atoms at the surface than in the bulk of the crystal. As a consequence, the magnetic moment of the Pt atoms which is induced by the Co atoms is reduced at the surface.

A very interesting aspect of the magnetic signals of Fig. 4 is their sensitivity to changes in both structural and magnetic parameters. This is particularly true in the minimum of the $(1,0,L)$ rod at $L \approx 3.5$ where the value of R is sensitive to changes in ns_m and also to

small changes in the surface atomic concentrations and relaxations. This high sensitivity of the R values along the diffraction rods seems a promising tool to characterize in detail the magnetism at surfaces.

To summarize, we have performed experiments of magnetic surface x-ray diffraction by measuring the magnetic asymmetry ratio R for surface reflections from $Co_3Pt(111)$. The resonant effect in R has been brought to evidence in the L_{III} absorption edge of Pt. The numerical values of R along diffraction rods allows us to conclude that the magnetism in the topmost Pt atoms is about one-half of that in the bulk atoms.

We wish to thank C. Vettier and R. van Silfhout for help in early experiments, R. Baudoing-Savois and Y. Gauthier for lending the crystal, P. Bernard for technical assistance, and Y. Petroff and M. Altarelli for critical reading of the manuscript.

[1] F. de Bergevin and M. Brunel, Phys. Lett. A **39**, 141 (1972).
[2] For a review, see I. K. Robinson, in *Handbook of Synchrotron Radiation*, edited by G. Brown and D. E. Moncton (North-Holland, Amsterdam, 1991), Vol. 3.
[3] D. Gibbs, D. R. Harsman, E. D. Isaacs, D. B. Mc Whan, D. Mills, and C. Vettier, Phys. Rev. Lett. **61**, 1241 (1988).
[4] C. Kao, J. B. Hastings, E. D. Johnson, D. P. Siddons, G. C. Smith, and G. A. Prinz, Phys. Rev. Lett. **65**, 373 (1990).
[5] N. Bernhoeft, A. Stunault, C. Vettier, F. de Bergevin, D. Gibbs, T. R. Thurston, S. M. Saphiro, J. B. Hastings, P. Dalmas, G. Helgesen, and O. Vogt, J. Magn. Magn. Mater. **140–144**, 1421 (1995).
[6] A. Fasolino, P. Carra, and M. Altarelli, Phys. Rev. B **47**, 3877 (1993).
[7] G. M. Watson, D. Gibbs, G. H. Lander, B. D. Gaulin, L. E. Berman, H. Matzke, and W. Ellis, following Letter, Phys. Rev. Lett. **77**, 751 (1996).
[8] S. Ferrer and F. Comin, Rev. Sci. Instrum. **66**, 1674 (1995).
[9] G. Grubel, K. G. Huang, D. Gibbs, D. M. Zehner, A. R. Sandy, and S. G. J. Mochrie, Phys. Rev. B **48**, 18 119 (1993).
[10] Y. Gauthier, R. Baudoing-Savois, J. J. W. M. Rosink, and M. Sotto, Surf. Sci. **297**, 193 (1993).
[11] J. P. Hannon, G. T. Trammell, M. Blume, and D. Gibbs, Phys. Rev. Lett. **61**, 1245 (1988).
[12] F. de Bergevin, M. Brunel, R. M. Galera, V. Vettier, E. Elkaim, M. Bessiere, and S. Lefebvre, Phys. Rev. B **46**, 10 772 (1992).
[13] W. Bambinek, B. Craseman, R. W. Fink, U. H. Freund, H. Mark, C. D. Swift, R. E. Pierce, and P. V. Rao, Rev. Mod. Phys. **44**, 716 (1972).